UNIVERSIDAD DE LA REPÚBLICA
Facultad de Ciencias Económicas y de Administración
Instituto de Estadística

Inferencia Bayesiana para el análisis estadístico de datos de fatiga de materiales metálicos

Ivo Babuška, Zaid Sawlan, Marco Scavino, Barna Szabó, Raúl Tempone

Marzo 2016

Documentos de Trabajo

Serie DT (16 / 01) - ISSN : 1688-6453

Inferencia Bayesiana para el análisis estadístico de datos de fatiga de materiales metálicos

Ivo Babuška [1]
The University of Texas at Austin, ICES, USA.

Zaid Sawlan [2]
King Abdullah University of Science and Technology (KAUST), CEMSE, Saudi Arabia.

Marco Scavino [3]
Instituto de Estadística - Facultad de Ciencias Económicas y de Administración - UdelaR.

Barna Szabó [4]
Washington University in St. Louis, USA.

Raúl Tempone [5]
King Abdullah University of Science and Technology (KAUST), CEMSE, Saudi Arabia.

RESUMEN

Este trabajo está basado en el artículo *Bayesian inference and model comparison for metallic fatigue data*, con I. Babuška, Z. Sawlan, B. Szabó y R. Tempone, publicado en `https://arxiv.org/abs/1512.01779`.

En este trabajo exponemos un tratamiento estadístico de datos extraídos de un conjunto de registros de experimentos de fatiga que se realizaron en las aleaciones de aluminio 75S-T6.

Nuestro objetivo principal es predecir la vida de fatiga de materiales, proporcionando un enfoque sistemático para la calibración y clasificación de los modelos propuestos con referencia a los datos de fatiga. A tal efecto, consideramos varios modelos estadísticos con límite de fatiga y con límite de fatiga aleatorio adecuados para el tratamiento de datos censurados a la derecha.

En primer lugar, ajustamos los modelos a los datos por el método de máxima verosimilitud y estimamos las cuantías de la distribución de vida de las aleaciones. La robustez

[1] `babuska@ices.utexas.edu`
[2] `zaid.sawlan@kaust.edu.sa`
[3] `mscavino@iesta.edu.uy`
[4] `barna.szabo@esrd.com`
[5] `raul.tempone@kaust.edu.sa`

de dichas estimaciones es evaluada por medio de intervalos de confianza obtenidos con una técnica de remuestreo estratificado respecto del ciclo de carga repetida. Una primera clasificación de los modelos adoptados es llevada a cabo a través de medidas clásicas de ajuste basadas en criterios de información.

En segundo lugar, ampliamos el alcance de nuestro estudio considerando un enfoque Bayesiano. Dado el escenario a priori seleccionado por el usuario para incorporar el conocimiento disponible sobre los parámetros físicos de interés, se obtienen las distribuciones a posteriori aproximadas de dichos parámetros basadas en técnicas de simulación. Para clasificar los modelos Bayesianos y determinar qué modelo sería preferible para un determinado escenario a priori, hemos aplicado tanto métodos basados en la estimación de la verosimilitud marginal como en modernos criterios de información de tipo predictivo, cuya aplicación requiere el uso de técnicas de validación cruzada.

Palabras claves: Datos de fatiga, predicción de vida de fatiga, modelos con límite de fatiga aleatorio, calibración y clasificación de modelos Bayesianos, precisión predictiva de modelos Bayesianos.

Clasificación MSC2010: 62N05, 62N01, 62P30, 62F15.

1. Introduction

Mechanical and structural components subjected to cyclic loading are susceptible to cumulative damage and eventual failure through an irreversible process called metal fatigue. Prediction of such fatigue through the expected service life of mechanical parts and assemblies is an important objective of numerical simulations used in mechanical and structural engineering practice. Based on such predictions, inspection intervals can be established. The frequency of these inspection intervals bears on the safety and costs of operation Schijve (2003, 2009); Fatemi and Yang (1998).

The fatigue characteristics of materials are established through fatigue tests performed on coupons, also called dogbone specimens, made of round bars or flat plates. The coupons are designed such that the stress is highest in the gauge section and that it remains substantially constant when the coupon is loaded in the axial direction. In bending and torsion tests, the stress varies linearly over the cross section and is constant in the axial direction, for any fixed point in the cross section.

The number of cycles to failure, the peak stress and the cycle ratio are recorded for each experiment. The cycle ratio is defined as the minimum stress to maximum stress ratio. When an experiment is stopped before the specimen fails, then the test record is marked as a run-out. In some experiments, the specimen may buckle or fail outside of the gauge section. Such experiments are disregarded. State-of-the-art reviews on mechanical fatigue are presented in Schijve (2003) and Fatemi and Yang (1998). Here, we focus on high-cycle (stress-life) fatigue.

The set of data pairs (S_i, N_i), where S_i is the stress and N_i is the corresponding number of cycles at failure in the ith test, exhibits substantial statistical dispersion. Interpretation and generalization of test data are essential for making risk-informed design decisions. The goal is to find a probability distribution for the fatigue life given data and underlying assumptions. There are many possible phenomenological models which will lead to different results. These results can be derived by different statistical frameworks, among them the frequentist and the Bayesian approaches. Furthermore, there are several ways to judge the results obtained by the use of different models. Various statistical models such as lognormal, extreme value, Weibull and Birnbaum-Saunders distributions have been used for this purpose.

We consider different types of models that contain fatigue limit parameters. Although such models have been widely used (see, for example, Rice et al. (2003); Pascual and Meeker (1997, 1999); Ryan (2003)), there is an ongoing debate concerning the existence of the fatigue limit Pyttel et al. (2011); Bathias (1999). Some authors use the terms "endurance limit" or "fatigue strength" instead of "fatigue limit" Schijve (2003); Pascual and Meeker (1999). We distinguish between the fatigue limit, which is a physical notion, and the fatigue limit parameter, which is an unknown parameter, expressed in the same scale as the equivalent stress and calibrated for different models. Usually, data support curve fitting up to a certain number of cycles to failure only. Extrapolation beyond that number substantially increases uncertainty. For example, aluminum does not have a fatigue limit, since it will always fail if tested to a sufficient number of cycles. Therefore, the fatigue limit (fatigue strength) of aluminum is reported as the stress level at which the material can survive after a large number of cycles. For the purposes of this paper, the number of cycles can be fixed at 2×10^7, since the available data do not contain substantially larger cycle values.

We employ a classical (likelihood-based) approach to fit and compare the proposed models using the 75S-T6 aluminum sheet specimen data set described in Section 2. Ultimately, we provide an analog Bayesian approach to fit and compare the models. The classical approach provides a point estimation (Maximum Likelihood estimate) for the model parameter θ that lies in the 90 % confidence interval if it were repeatedly used with random data from the model for fixed θ. In the Bayesian formulation, no repetition is required and the interval estimation is based on the posterior distribution. Although Ryan used a Bayesian approach to find an optimal design for the random fatigue-limit model Ryan (2003), we are, to our knowledge, the first to use Bayesian methods to analyze and compare fatigue models.

The remainder of this paper is organized as follows. Section 2 introduces the main characteristics of the fatigue tests conducted at the Battelle Memorial Institute on 85 75S-T6 aluminum sheet specimens by means of a Krouse direct repeated-stress testing machine. The data set with the fatigue test results is available as a csv file in the supplemental material to this paper. This data set contains run-outs. Section 3 presents classical statistical models of fatigue test results. In Subsection 3.1, we first consider a classical statistical fitting technique, called logarithmic fit, for illustration purposes only, that does not take in to account the presence of run-outs. Subsequently, we introduce fatigue-limit models and random fatigue-limit models, which are both specially designed to fit data in the presence of run-outs. We fit two fatigue-limit models, whose mean value function is same as in the logarithmic fit, with constant and non-constant variance functions, by constructing the corresponding likelihood functions and estimating all the unknown parameters that define the S-N curves by means of the maximum likelihood method. The fatigue limit parameter assessment under both models can be done by computing numerically tailored functions from their joint likelihoods, usually called profile likelihoods Pawitan (2001). Later, we extend these models by assuming that the fatigue limit parameter is a random variable. To clarify the fitting procedure that provides estimates for S-N curves and predictions of fatigue life, we consider two random fatigue-limit models and their extensions, where a non-constant variance function is used. The assessment of the fatigue limit parameter is then summarized by comparing the estimated probability density functions of the four fitted models. Subsection 3.2 includes the computation of bootstrap confidence bands for the S-N curves and bootstrap confidence intervals for the maximum likelihood estimates. Subsection 3.3 is dedicated to comparison of the models by some widely used information criteria. Section 4 focuses on the Bayesian analysis of some of the models. In Subsection 4.1, three of the models analyzed using the likelihood approach are embedded in a Bayesian framework that we characterize based on informative priors. We use Bayesian computational techniques to estimate the posterior probability density function of each individual parameter of the six fitted models as well as the bivariate posterior probability functions of all the combinations of two parameters out of the total number of parameters for any of the six fitted models. Subsection 4.2 presents the Bayesian model comparison approach, which includes the Bayes factor and predictive information criteria. The Bayes factor is approximated by means of the Laplace method and the Laplace-Metropolis method. The Bayes factor is used to evaluate the fit of Bayesian models while the predictive information criteria are used to compare models based on their predictive accuracy.

2. The 75S-T6 aluminum sheet specimens data set

Data are available from 85 fatigue experiments that applied constant amplitude cyclic loading to unnotched sheet specimens of 75S-T6 aluminum alloys (Grover et al., 1951, table 3, pp.22–24). The following data are recorded for each specimen:

- the maximum stress, S_{max}, measured in ksi units.
- the cycle ratio, R, defined as the minimum to maximum stress ratio.
- the fatigue life, N , defined as the number of load cycles at which fatigue failure occurred.
- a binary variable (0/1) to denote whether or not the test had been stopped prior to the occurrence of failure (run-out).

In 12 of the 85 experiments, the specimens remained unbroken when the tests were stopped. The recorded number of load cycles for these 12 experiments is the lower bound of an interval in which failure would have occurred had the test been continued. If specimens buckled or failed outside the test section, they are not included in the data set.

3. Classical approach

3.1. Model calibration

There are many linear and nonlinear models (S-N curves) that have been used to predict fatigue life, N, in terms of the stress, S. A good list of these models can be found in Castillo and Fernández-Canteli (2009). In this section, we consider relevant nonlinear regression models used with the 75S-T6 data set. For the sake of completeness, we first show how the fitting procedure works for a model that does not take into account the run-out feature of some observations. This so-called "equivalent stress equation model" was used in Rice et al. (2003). Secondly, we introduce some fatigue-limit models that are tailored to work well in the presence of run-out observations, similar to Pascual and Meeker (1997) and Pascual and Meeker (1999), and we calibrate each of these models by using the maximum likelihood method.

In all the proposed models, the quantities of interest are the prediction of fatigue life, given the test stress and the cycle ratio, and the estimation of the fatigue limit parameter. The fatigue life predictions are summarized by means of the quantile functions. We plot the median (S-N curve), the 0.95 quantile and the 0.05 quantile.

Prior to the fitting of any statistical model, the fatigue data obtained for particular cycle ratios need to be generalized to arbitrary cycle ratios. For this purpose, the equivalent stress, S_{eq}, is then defined as $S_{eq}^{(q)} = S_{max}\,(1-R)^q$, where q is a fitting parameter. This definition is also used in Rice et al. (2003) and Walker (1970).

We first consider the logarithmic fit as defined in Szabó (2012) and Rice et al. (2003); that is,

$$\mu(S_{eq}^{(lg)}) = A_1 + A_2 \log_{10}(S_{eq}^{(lg)} - A_3), \tag{1}$$

using the objective function proposed in (Szabó (2012)),

$$e_{\text{std}} = \left(\frac{\sum_{i=1}^{n} (\log_{10}(n_i) - \mu(S_{eq}^{(lg)}))^2}{n-p} \right)^{1/2}, \tag{2}$$

where n is the number of data points and p is the number of fitting parameters (namely A_1, A_2, A_3 and q).

The resulting estimated mean value function is given by

$$\mu(S_{eq}^{(lg)}) = 10.07 - 3.54\ \log_{10}(S_{eq}^{(lg)} - 25.41)\,,$$

where $S_{eq}^{(lg)} = S_{max}\,(1-R)^{0.5147}$ and the value of the objective function is $e_{std} = 0.5195$.

Remark. Run-outs will introduce a bias error in the estimate when this approach is used. The resulting estimated mean value function, without the run-outs, is given by

$$\mu(S_{eq}^{(lg)}) = 7.71 - 2.17\ \log_{10}(S_{eq}^{(lg)} - 31.53)\,,$$

where $S_{eq}^{(lg)} = S_{max}\,(1-R)^{0.4633}$ and the value of the objective function is $e_{std} = 0.3673$. Clearly, removing the run-outs increases the value of the fatigue limit. Figure 1 shows the estimated quantile functions for the logarithmic fit, with the estimated fatigue limit parameter equal to 31.53 ksi. We point out that the estimated fatigue limit is equal to $31.53/(2^{0.4633}) = 22.87$ ksi, since the fatigue limit is the value of the maximum stress when the cycle ratio, R, is equal to -1 (the "fully reversed" condition).

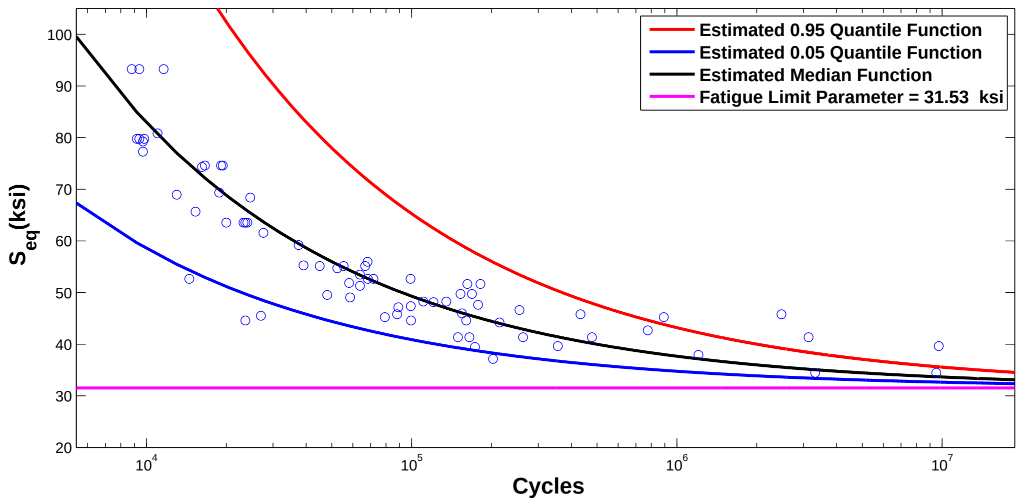

Figura 1: Logarithmic fit of the 75S-T6 data set without run-outs. The fatigue life prediction increases toward infinity as the equivalent stress, S_{eq}, tends to the estimated fatigue limit parameter (horizontal asymptote) for any estimated quantile function.

3.1.1. Model Ia

Let A_3 be the fatigue limit parameter. At each equivalent stress with $S_{eq} > A_3$, the fatigue life, N, is modeled by means of a lognormal distribution. This implies that $\log_{10}(N)$ is modeled with a normal distribution with mean $\mu(S_{eq})$ and standard deviation $\sigma(S_{eq})$. We generalize the logarithmic fit by assuming that

- $\mu(S_{eq}) = A_1 + A_2 \, \log_{10}(S_{eq} - A_3)\,, \;$ if $\; S_{eq} > A_3$
- $\sigma(S_{eq}) = \tau\,.$

Moreover, the model is now properly tailored to include the available censored fatigue data (run-outs). Given the sample data, $\mathbf{n} = (n_1, \ldots, n_m)$ and assuming that the observations are independent, the likelihood function is therefore given by

$$L(A_1, A_2, A_3, \tau, q; \mathbf{n}) = \prod_{i=1}^{m} \left[\frac{1}{n_i \log(10)} g(\log_{10}(n_i)\,; \mu(S_{eq})\,, \sigma(S_{eq})) \right]^{\delta_i} \left[1 - \Phi\left(\frac{\log_{10}(n_i) - \mu(S_{eq})}{\sigma(S_{eq})} \right) \right]^{1-\delta_i},$$

where $g(t; \mu, \sigma) = \frac{1}{\sqrt{2\pi}\,\sigma} exp\left\{ -\frac{(t-\mu)^2}{2\sigma^2} \right\}$, Φ is the cumulative distribution function of the standard normal distribution, and

$$\delta_i = \begin{cases} 1 & \text{if } n_i \text{ is a failure} \\ 0 & \text{if } n_i \text{ is a run-out}\,. \end{cases}$$

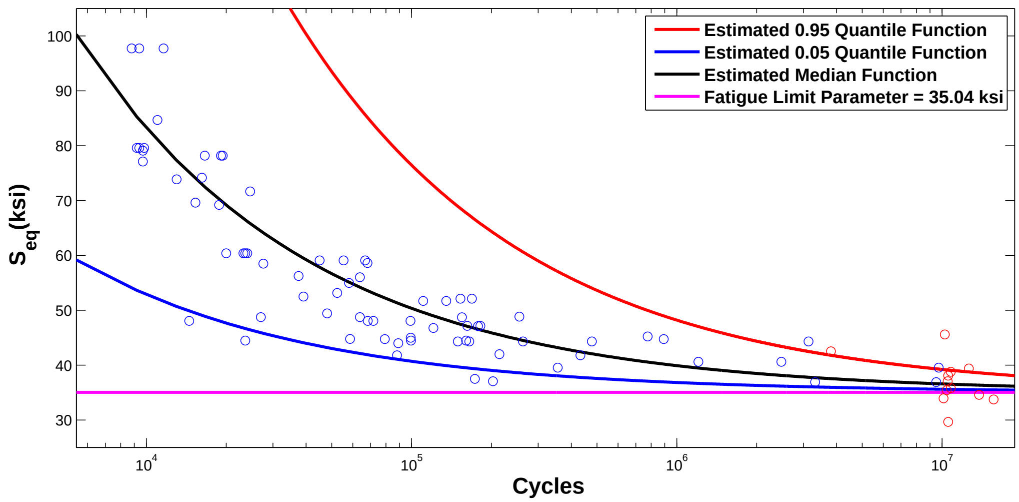

Figura 2: Model Ia fit of the 75S-T6 data set. Under the assumption that S_{eq} has constant variance, the addition of the run-outs (red circles) and fitting a model designed to handle right-censored data has the effect of enlarging the gap between the median and the 0.95 quantile (in the upper range of values of S_{eq}, the number of cycles to attain failure has substantially increased with respect to the logarithmic fit) and between the median and the 0.05 quantile (in the lower range of values of S_{eq}, the number of cycles to attain failure has decreased with respect to the logarithmic fit). The fatigue limit parameter estimate (purple line) is closer to the observed failures (blue circles) with smallest values of S_{eq} than the same estimate using the logarithmic fit (Figure 1).

This model is characterized by five parameters: $\theta = (A_1, A_2, A_3, q, \tau)$, whose maximum likelihood (ML) estimate, obtained by calibrating the model with the data, is

$$\mu(S_{eq}) = 7.38 - 2.01\, \log_{10}(S_{eq} - 35.04)\,,$$

where $S_{eq} = S_{max}\,(1-R)^{0.5628}$ and $\tau = 0.5274$. The maximum likelihood estimates are summarized in Table 1. The corresponding fit is shown in Figure 2 (blue circles = observed failures; red circles = run-outs). The difference between Model Ia and the logarithmic fit shows the importance of including the run-outs especially in the estimation of the fatigue limit. Run-outs that correspond to equivalent stress levels greater than the fatigue limit parameter are called significant run-outs. Only significant run-outs contribute to estimating the parameters. In this case, eight of the 12 run-outs were significant.

Cuadro 1: Maximum likelihood estimates for Model Ia

	A_1	A_2	A_3	q	τ
Model Ia	7.38	-2.01	35.04	0.5628	0.5274

3.1.2. Model Ib

We extend the model proposed in Subsection 3.1.1 by allowing a non-constant standard deviation as in Pascual and Meeker (1997):

- $\mu(S_{eq}) = A_1 + A_2 \log_{10}(S_{eq} - A_3)\,,$ if $S_{eq} > A_3$
- $\sigma(S_{eq}) = 10^{(B_1 + B_2 \log_{10}(S_{eq}))}\,,$ if $S_{eq} > A_3$

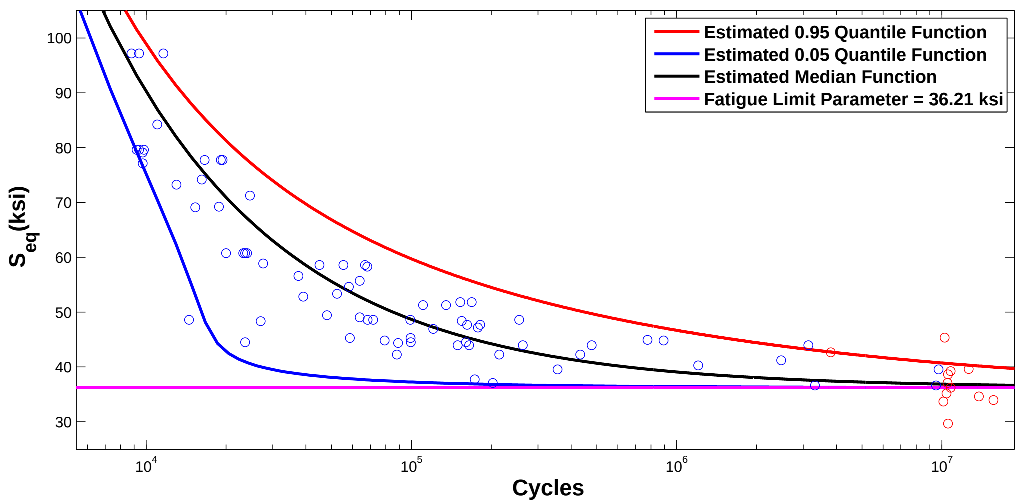

Figura 3: Model Ib fit of the 75S-T6 data set. Allowing non-constant variance of S_{eq} in a censored data model has the effect of reducing the gap between the median and both the 0.95 and 0.05 quantiles along the upper range of values of S_{eq}. In the case of the lower range of values of S_{eq}, the gap between the median and the 0.05 quantile has increased with respect to the Model Ia fit (Figure 2). The estimate of the fatigue limit parameter is very close to the minimum value of S_{eq} that leads to failure. The estimated fatigue limit is 24.71 ksi.

In this model, there are six parameters: $\theta = (A_1, A_2, A_3, q, B_1, B_2)$, and their ML estimates are

$$\mu(S_{eq}) = 6.72 - 1.57\ \log_{10}(S_{eq} - 36.21),$$
$$\sigma(S_{eq}) = 10^{(4.55 - 2.89\log_{10}(S_{eq}))},$$

where $S_{eq} = S_{max}\,(1-R)^{0.5510}$. The maximum likelihood estimates are summarized in Table 2. The corresponding fit is shown in Figure 3 (blue circles = observed failures; red circles = run-outs). Figure 3 shows that the uncertainty in predicting fatigue life decreases with high values of the equivalent stress when compared to Model Ia. However, the uncertainty increases for values of the equivalent stress that are close to the estimated fatigue limit parameter. In Model Ib, there are seven significant run-outs because the fatigue limit parameter has increased to 36.21 ksi. When $A_3 < S_{eq} < 100$, the estimated standard deviation ranges between 1.11 and 0.059 , supporting the assumption of a non-constant standard deviation.

Cuadro 2: Maximum likelihood estimates for Model Ib

	A_1	A_2	A_3	q	B_1	B_2
Model Ib	6.72	-1.57	36.21	0.5510	4.55	-2.89

Remark. **Profile likelihoods**. To assess the plausibility of a range of values of the fatigue limit parameter, A_3, we construct the profile likelihood (Pascual and Meeker, 1997, p. 294):

$$R(A_3) = \max_{\theta_0}\left[\frac{L(\theta_0, A_3)}{L(\hat{\theta})}\right], \tag{3}$$

where θ_0 denotes all parameters except for the fatigue limit parameter, A_3, and $\hat{\theta}$ is the ML estimate of θ.

Figure 4 shows the profile likelihood functions for A_3 corresponding to the models in Subsections 3.1.1 and 3.1.2. As in Pascual and Meeker (1997), approximate $100(1-\alpha)\,\%$ confidence intervals for A_3 based on the calibrated profile likelihoods are given by: $\{A_3 : -2\log(R(A_3)) \leq \chi^2_{1;1-\alpha}\}$, where $\chi^2_{1;1-\alpha}$ is the $100(1-\alpha)$ percentile of a chi-square distribution with 1 degree of freedom. The approximate 95 % confidence intervals for A_3 are $(32.45, 36.28)$ and $(34.36, 36.88)$ for models Ia and Ib, respectively. We can see that each model suggests a different range for the fatigue limit parameter, A_3. We therefore need to systematically choose which model is better to assess the value of A_3.

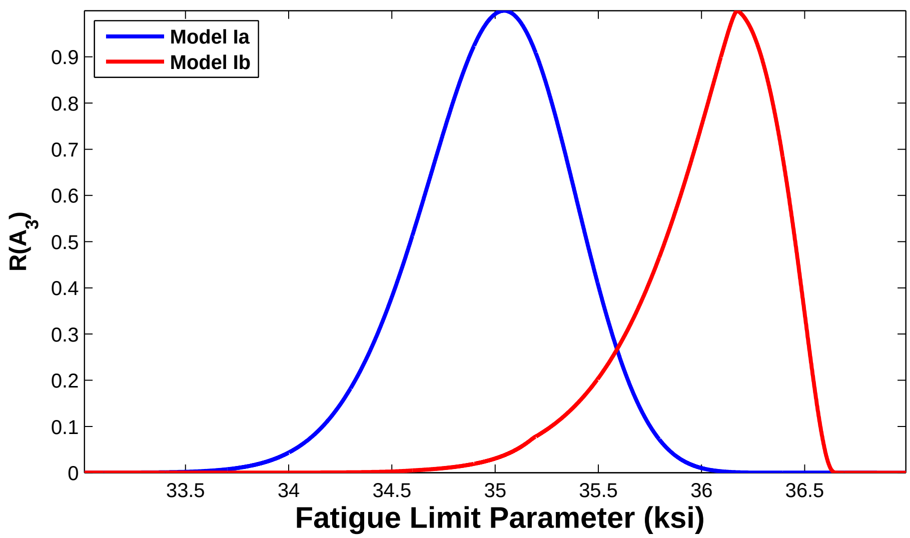

Figura 4: Profile likelihood estimates for the fatigue limit parameter, A_3, with Model Ia fit (blue curve) and Model Ib fit (red curve). The two fitted fatigue-limit models display different ranges for the most plausible values of the fatigue limit parameter, A_3, a feature that is amplified by the left-skewed profile likelihood under Model Ib.

3.1.3. Model IIa

We now extend the model proposed in Subsection 3.1.1 to allow a random fatigue limit parameter as in Pascual and Meeker (1999) :

- $\mu(S_{eq}) = A_1 + A_2 \log_{10}(S_{eq} - A_3)$, if $S_{eq} > A_3$.
- $\sigma(S_{eq}) = \tau$.
- $\log_{10}(A_3) \sim N(\mu_f, \sigma_f)$.

Here, we assume that $\log_{10}(N)$ given $A_3 < S_{eq}$ is modeled with a normal distribution with mean $\mu(S_{eq})$ and standard deviation $\sigma(S_{eq})$. In this case, the probability density function (pdf) of $\log_{10}(N)$ is obtained by marginalizing A_3:

$$f_{\log_{10}(N)}(u\,;\theta) = \int_0^{S_{eq}} h(u\,;\mu(S_{eq})\,,\sigma(S_{eq}))\,\ell_{A_3}(w\,;\mu_f\,,\sigma_f)\,dw\,,$$

where $\theta = (A_1, A_2, \mu_f, \sigma_f, q, \tau)$, $h(u\,;\mu(S_{eq})\,,\sigma(S_{eq}))$ is the conditional density of $\log_{10}(N)$ given A_3, and $\ell_{A_3}(w\,;\mu_f\,,\sigma_f)$ is the marginal density of A_3. Similarly, the marginal cumulative distribution function (cdf) of $\log_{10}(N)$ is given by

$$F_{\log_{10}(N)}(u\,;\theta) = \int_0^{S_{eq}} \Phi\left(\frac{u-\mu(S_{eq})}{\sigma(S_{eq})}\right)\,\ell_{A_3}(w\,;\mu_f\,,\sigma_f)\,dw\,,$$

where Φ is the conditional cumulative distribution function of $\log_{10}(N)$ given A_3. The functions $f_{\log_{10}(N)}$ and $F_{\log_{10}(N)}$ no longer have closed forms and must be numerically evaluated. Global adaptive quadrature is used to approximate the integrations (see Shampine (2008)).
Assuming independent observations, the likelihood function of $\theta = (A_1, A_2, \mu_f, \sigma_f, q, \tau)$ is therefore given by

$$L(\theta; \{\log_{10}(n_1), \ldots, \log_{10}(n_m)\}) = \prod_{i=1}^{m} \left[f_{\log_{10}(N)}(\log_{10}(n_i)\,;\theta)\right]^{\delta_i} \left[1 - F_{\log_{10}(N)}(\log_{10}(n_i)\,;\theta)\right]^{1-\delta_i}, \tag{4}$$

where

$$\delta_i = \begin{cases} 1 & \text{if } n_i \text{ is a failure} \\ 0 & \text{if } n_i \text{ is a run-out}\,. \end{cases}$$

3.1.4. Model IIb

We can also consider a random fatigue-limit model with the smallest extreme value (sev) distribution as in Pascual and Meeker (1999):

- $\mu(S_{eq}) = A_1 + A_2 \log_{10}(S_{eq} - A_3)\,,$ if $S_{eq} > A_3$.
- $\sigma(S_{eq}) = \tau\,.$
- the density of $\log_{10}(A_3)$ is $\phi(t; \mu_f, \sigma_f)$.
- the conditional density of $\log_{10}(N)$ given $A_3 < S_{eq}$ is $\phi(t; \mu(S_{eq}), \sigma(S_{eq}))\,,$

where $\phi(t; \mu, \sigma) = \frac{1}{\sigma} exp\left\{\left(\frac{t-\mu}{\sigma}\right) - exp\left(\frac{t-\mu}{\sigma}\right)\right\}$ is the sev probability density function with location parameter μ and scale parameter σ (Meeker and Escobar, 1998, Chapter 4). The likelihood function has the same form as in equation (4). In other words, the conditional fatigue life, N, and the fatigue limit parameter, A_3, are modeled by a Weibull distribution. Table 3 shows the maximum likelihood estimates and the maximum likelihood values obtained for Model IIa and Model IIb. The estimated parameters for both models are similar except for the parameters, σ_f and τ, which have smaller values with Model IIb. As a consequence, Model IIb has a smaller maximum likelihood value. Since models IIa and IIb have the same number of parameters, we can conclude that Model IIb is better than Model IIa. It is thus sufficient to present the corresponding fit of Model IIb (Figure 5).
Figure 6 shows the probability density function for A_3 corresponding to models IIa and IIb.
In the next subsections, our goal is to compare the relative performances of the proposed models that include an adequate formulation in terms of run-outs. As an initial step, we

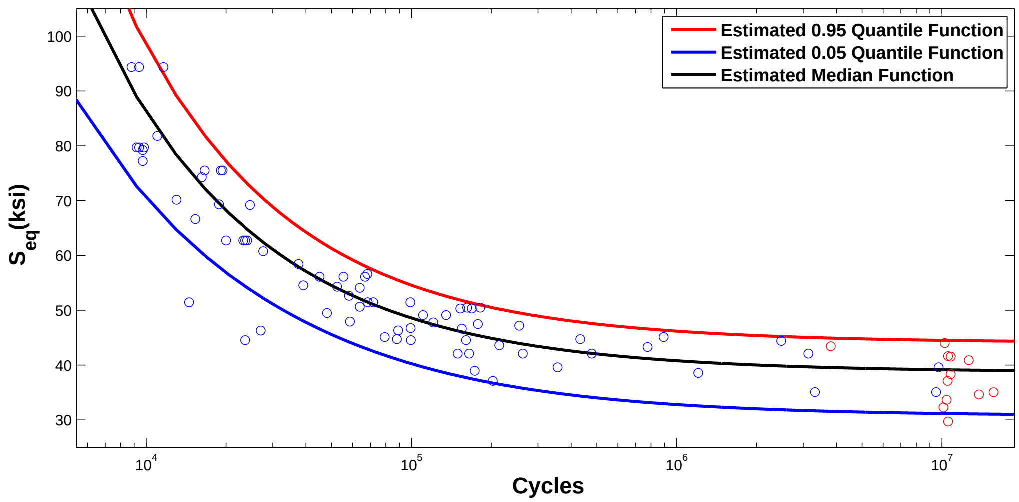

Figura 5: Model IIb fit of the 75S-T6 data set. The fitting of a random fatigue-limit model for censored data has the effect that the estimated quantiles converge fast to an horizontal asymptote. Unlike fatigue-limit models, the random fatigue-limit model has the property that each estimated quantile approaches a different horizontal asymptote.

Cuadro 3: Maximum likelihood estimates for Model IIa and Model IIb.

	A_1	A_2	μ_f	σ_f	q	τ	$\log(L^*)$
Model IIa	6.53	-1.51	1.58	0.0473	0.4888	0.1447	-913.42
Model IIb	6.51	-1.47	1.60	0.0385	0.4886	0.0852	-907.31

explore the consistency of the fitted models by looking at the variability in the confidence bands of the quantile functions of fatigue life.

3.2. Bootstrap confidence bands and confidence intervals

We obtain bootstrap confidence bands for the model fittings Ia, Ib and IIb, as illustrated in Figures 2, 3 and 5, respectively. Stratified bootstrap algorithm 1 is implemented with censored data. First, the data set is stratified on the basis of the cycle ratio, R. Then, we sample independently from each stratum where each sample contains S_{max}, R, N and the binary variable δ (see Efron (1981)). By repetition, we generate $M = 200$ bootstrap data sets. For each data set, we obtain the maximum likelihood estimate and compute the corresponding quantiles.

Figure 7 shows the median functions (blue curves) and the bootstrapped 95 % confidence

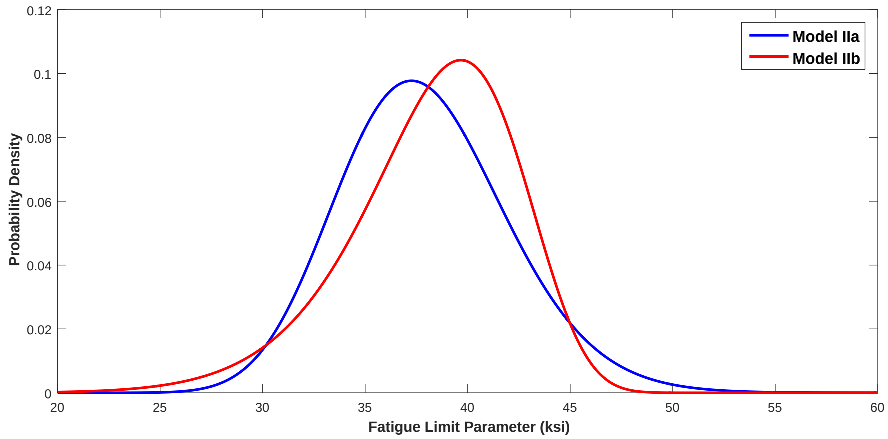

Figura 6: Estimated probability density functions of the fatigue limit parameter, A_3, for models IIa and IIb.

Algorithm 1 Stratified bootstrap algorithm for censored data

1: **set** $data = [data_1, data_2, \ldots, data_n]$
2: **for** $i = 1 : n$ **do**
3:     **draw** $|data_i|$ samples with replacement from $data_i$
4:     **let** $data_i^*$ be the bootstrap stratum.
5: **let** $data^* = [data_1^*, data_2^*, \ldots, data_n^*]$ be the bootstrap data set.
6: **find** the maximum likelihood estimate θ^* given $data^*$
7: **compute** the bootstrap quantiles
8: **repeat** steps (2 to 7) M times.

bands (black curves) for models Ia, Ib and IIb. Figure 8 shows the 0.05 quantiles (blue curves) and the bootstrapped 95 % confidence bands (black curves). Table 4 provides the bootstrap confidence intervals for the maximum likelihood estimates for these models. Clearly, the random fatigue-limit model (Model IIb) provide the narrowest confidence intervals for A_1, A_2 and q.

3.3. Model comparison

Using a classical approach, we compute some popular information criteria, such as Akaike information criterion (AIC) Akaike (1992), Bayesian information criterion (BIC) Schwarz (1978); Neath and Cavanaugh (2012) and AIC with correction Burnham and Anderson (2002), which are based on the maximized log-likelihood values. Such measures take into account both the goodness of fit and the complexity of the models in terms of the number

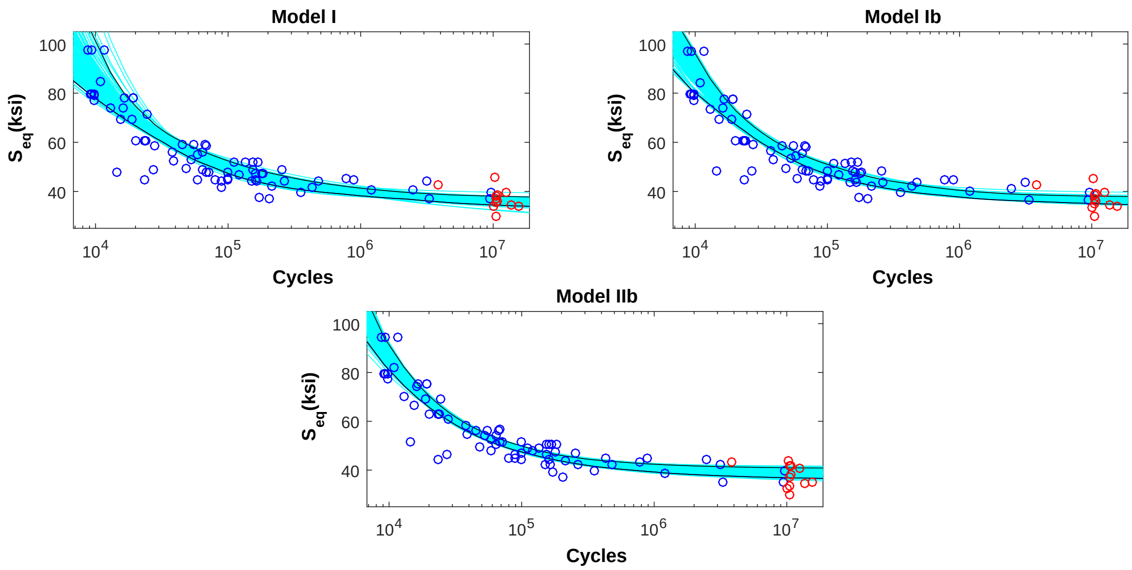

Figura 7: 95 % bootstrap confidence bands for the median of fatigue life.

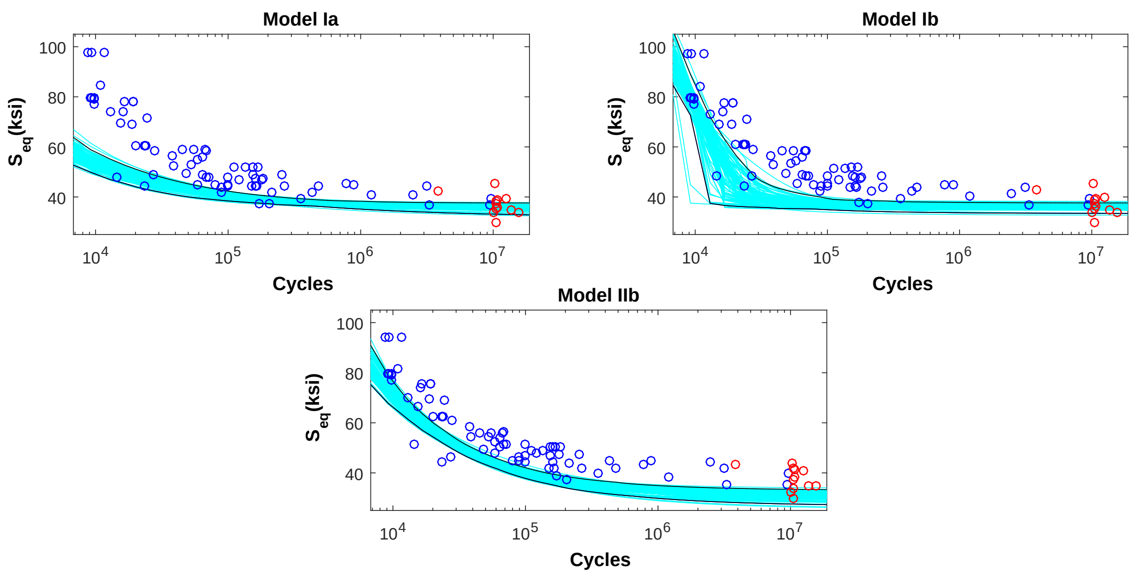

Figura 8: 95 % bootstrap confidence bands for the 0.05 quantile of fatigue life. The 0.05 quantile is not as robust as the median, especially for Model Ib.

of parameters.

Table 5 contains the maximum log-likelihood values that correspond to the models intro-

Cuadro 4: 95 % bootstrap confidence intervals for the maximum likelihood estimates.

Model Ia					
A_1	A_2	A_3	q	τ	
(6.19, 8.79)	(-2.88, -1.22)	(31.01, 38.46)	(0.487, 0.613)	(0.355, 0.646)	
Model Ib					
A_1	A_2	A_3	q	B_1	B_2
(6.28, 7.45)	(-2.05, -1.31)	(33.66, 38.33)	(0.460, 0.595)	(3.48, 6.25)	(-3.92, -2.31)
Model IIb					
A_1	A_2	μ_f	σ_f	q	τ
(6.23, 6.87)	(-1.70, -1.30)	(1.58, 1.62)	(0.0275, 0.0497)	(0.451, 0.515)	(0.035, 0.123)

duced in Subsections 3.1.1 – 3.1.4 together with the classical information criteria computations. These classical evaluations of model uncertainty indicate that, despite its complexity, Model IIb is preferable.

Cuadro 5: Classical information criteria show that Model IIb provides the best fit to the 75S-T6 data set.

Models	**Ia**	**Ib**	**IIa**	**IIb**
maximum log-likelihood	-950.16	-920.51	-913.42	-907.31
Akaike Information Criterion (AIC)	1910.3	1853.0	1838.8	1826.6
Bayesian Information Criterion (BIC)	1922.5	1867.7	1853.5	1841.3
Akaike Information Criterion with correction	1911.1	1854.1	1839.9	1827.7

4. Bayesian approach

4.1. Model calibration

We consider now a Bayesian approach to study models Ia, Ib and IIb under an informative priors scenario. We compute the maximum posterior estimate (analytically) using the Laplace method and provide Markov chain Monte Carlo (MCMC) posterior samples. The random walk Metropolis-Hastings algorithm (2) is used to generate MCMC samples. We use a normal proposal distribution to perturb the current simulated vector, θ_c, and generate a new perturbed vector, $\theta_p \sim N(\theta_c, diag(\delta))$, where δ is a vector of parameters that controls the acceptance rate of the algorithm. After several attempts, we chose δ

such that we could obtain a reasonable acceptance rate (see (Robert and Casella, 2009, Chapter 6)).

Algorithm 2 Random walk Metropolis-Hastings algorithm

1: **set** an initial value for the chain: $\theta_c = \theta_0$ and **choose** δ
2: **compute** $a = loglikelihood(\theta_c) + logprior(\theta_c)$
3: **draw** θ_p from $N(\theta_c, diag(\delta))$
4: **compute** $b = loglikelihood(\theta_p) + logprior(\theta_p)$
5: **let** $H = min(1, exp(b - a))$ and **draw** r from $U(0, 1)$
6: **if** $H > r$ **then**
7: $\quad\theta_c = \theta_p$
8: $\quad a = b$
9: **repeat** steps (3 to 8) **until** L posterior samples are attained.

The algorithm is initialized as follows:

- Model Ia: $\theta_0 = (7.4, -2, 35, 0.56, 0.5)$ and $\delta = (0.1, 0.1, 0.1, 0.01, 0.05)$.
- Model Ib: $\theta_0 = (6.7, -1.6, 36.2, 0.55, 4.6, -2.9)$ and $\delta = (0.1, 0.1, 0.1, 0.01, 0.1, 0.1)$.
- Model IIb: $\theta_0 = (6.5, -1.5, 1.6, 0.04, 0.49, 0.085)$ and $\delta = (0.1, 0.1, 0.005, 0.001, 0.01, 0.01)$.

Each chain was run for $1,010,000$ times, with a 10,000 iterations burn-in period and every 50th draw of the chain kept. The MCMC posterior samples were summarized by the Laplace-Metropolis estimator (see Lewis and Raftery (1997)), the empirical mean and standard deviation and the estimated marginal densities. The marginal densities were obtained by kernel density estimation (KDE) with a normal kernel function. The bandwidth was chosen to be optimal for normal densities.
In attempting to provide an objective Bayesian analysis, we considered two different scenarios (see our original paper *Bayesian inference and model comparison for metallic fatigue data*, Computer Methods in Applied Mechanics and Engineering, vol.304 (2016), pp.171-196) by choosing data-dependent proper priors Berger (2006). Here we describe only the informative priors scenario, where normal priors centered around the maximum likelihood estimates with arbitrary variance were considered for all the parameters except the standard deviations that were assigned inverse-gamma priors.

4.1.1. Informative priors scenario

We considered the following informative priors that were induced from the maximum likelihood estimates as explained previously.

- Model Ia: $A_1 \sim \mathcal{N}(7.4, 2)$, $A_2 \sim \mathcal{N}(-2, 2)$, $A_3 \sim \mathcal{N}(35, 2)$, $q \sim \mathcal{N}(0.56, 0.5)$, $\tau \sim$ Inv-Gamma$(0.5, 0.25)$.
- Model Ib: $A_1 \sim \mathcal{N}(6.7, 2)$, $A_2 \sim \mathcal{N}(-1.6, 2)$, $A_3 \sim \mathcal{N}(36.2, 2)$, $q \sim \mathcal{N}(0.55, 0.5)$, $B_1 \sim \mathcal{N}(4.6, 2)$, $B_2 \sim \mathcal{N}(-2.9, 2)$.
- Model IIb: $A_1 \sim \mathcal{N}(6.5, 2)$, $A_2 \sim \mathcal{N}(-1.5, 2)$, $\mu_f \sim \mathcal{N}(1.6, 0.1)$, $\sigma_f \sim$ Inv-Gamma$(2, 0.1)$, $q \sim \mathcal{N}(0.49, 0.5)$, $\tau \sim$ Inv-Gamma$(1, 0.1)$.

Numerical Results - Model Ia

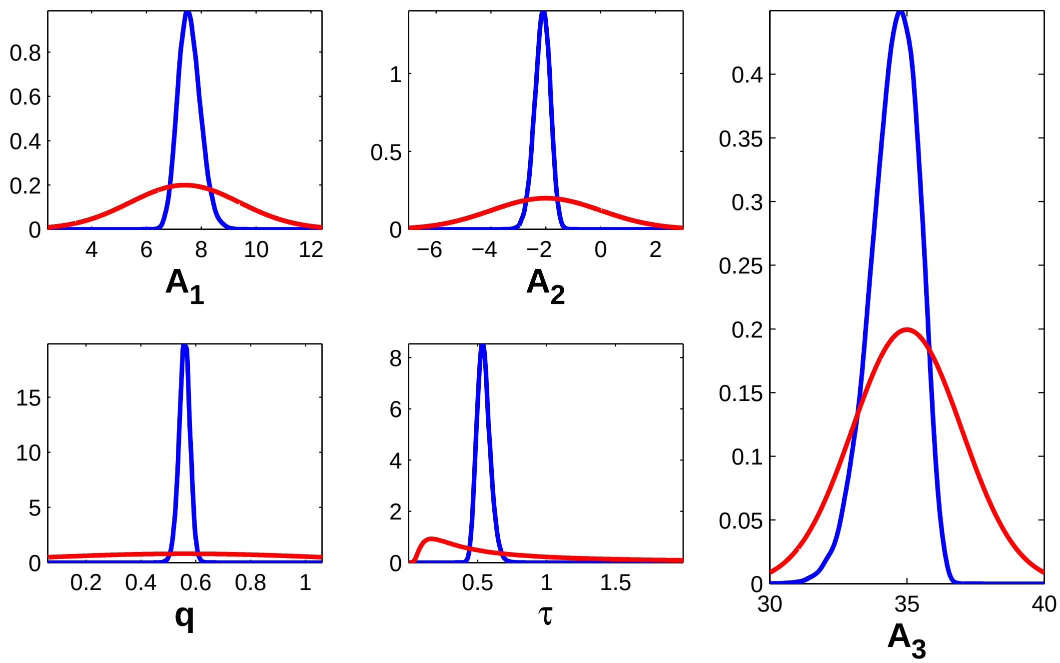

Figura 9: Prior densities (red line) and approximate marginal posterior densities (blue line) for A_1, A_2, q, τ and A_3. The marginal posterior densities for all parameters are highly concentrated around their unique mode, suggesting that the observed data, given the assumed model, considerably increase our degree of belief about the range of the parameters. The high concentrations of q and τ are especially noticeable. The estimated marginal posterior of the fatigue limit parameter, A_3, is left-skewed although the prior was assumed to be a normal distribution.

Maximum posterior estimates shown in Table 6 are similar to the maximum likelihood estimates obtained for Model Ia (Table 1). Figure 9 and empirical standard deviations

Cuadro 6: Maximum posterior estimates for Model Ia.

Estimator	A_1	A_2	A_3	q	τ
Laplace	7.39	-2.01	35.03	0.563	0.523
Laplace-Metropolis	7.46	-2.07	34.92	0.561	0.524

Cuadro 7: MCMC posterior empirical mean estimates with their standard deviations.

	A_1	A_2	A_3	q	τ
Mean	7.57	-2.13	34.53	0.559	0.544
SD	0.41	0.28	0.88	0.020	0.048

given in Table 7 show that the fatigue limit parameter, A_3, is the most uncertain parameter whereas q is the least uncertain parameter. Figure 9 also shows that the data are informative for all the parameters because there is a contraction between the prior densities and the posterior densities. Correlation coefficients presented in Table 8 and Figure 10 show that A_1 and A_2 are approximately linear dependent. We can therefore reduce the number of parameters in Model Ia by one parameter. These parameters are also highly correlated with the fatigue limit parameter, A_3. On the other hand, there is a weak linear relationship between q and the parameters A_1, A_2 and A_3. Moreover, the standard deviation, τ, has no notable correlation with any parameter.

Cuadro 8: Correlation coefficients for each pair of parameters in Model Ia.

	A_1	A_2	A_3	q
A_2	-0.980	—	—	—
A_3	-0.860	0.799	—	—
q	-0.385	0.365	0.384	—
τ	-0.005	0.003	0.050	0.073

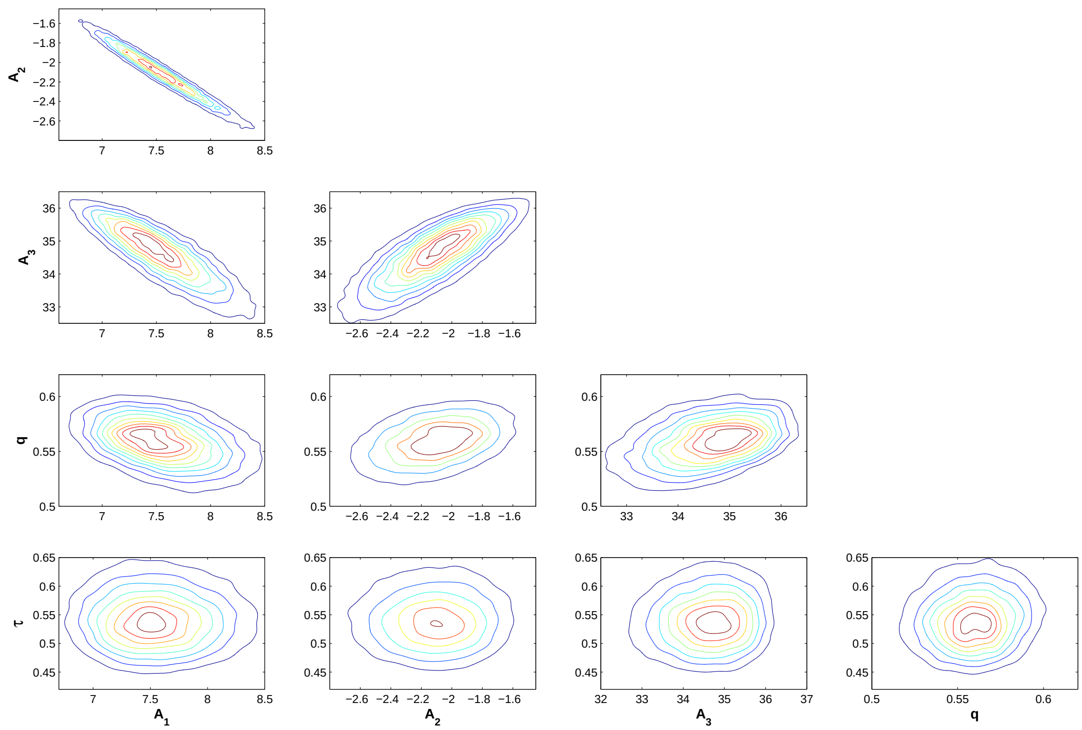

Figura 10: Contour plots of the estimated bivariate densities for each pair of parameters in Model Ia. A strong correlation appears between A_1 and A_2 and they also appear to be linearly dependent. The fatigue limit parameter, A_3, is highly correlated with A_1 and A_2.

Numerical Results - Model Ib

Cuadro 9: Maximum posterior estimates for Model Ib.

Estimator	A_1	A_2	A_3	q	B_1	B_2
Laplace	6.72	-1.57	36.21	0.551	4.56	-2.89
Laplace-Metropolis	6.78	-1.61	36.20	0.552	4.43	-2.83

Maximum posterior estimates given in Table 9 are similar to the maximum likelihood estimates obtained for Model Ib (Table 2). Similarly to Model Ia, Figure 11 and Table 10 show that the fatigue limit parameter, A_3, is the most uncertain parameter whereas q is the least uncertain parameter. However, the uncertainties have been reduced for A_1, A_2 and A_3 when compared with Model Ia. Figure 11 shows again that the data are

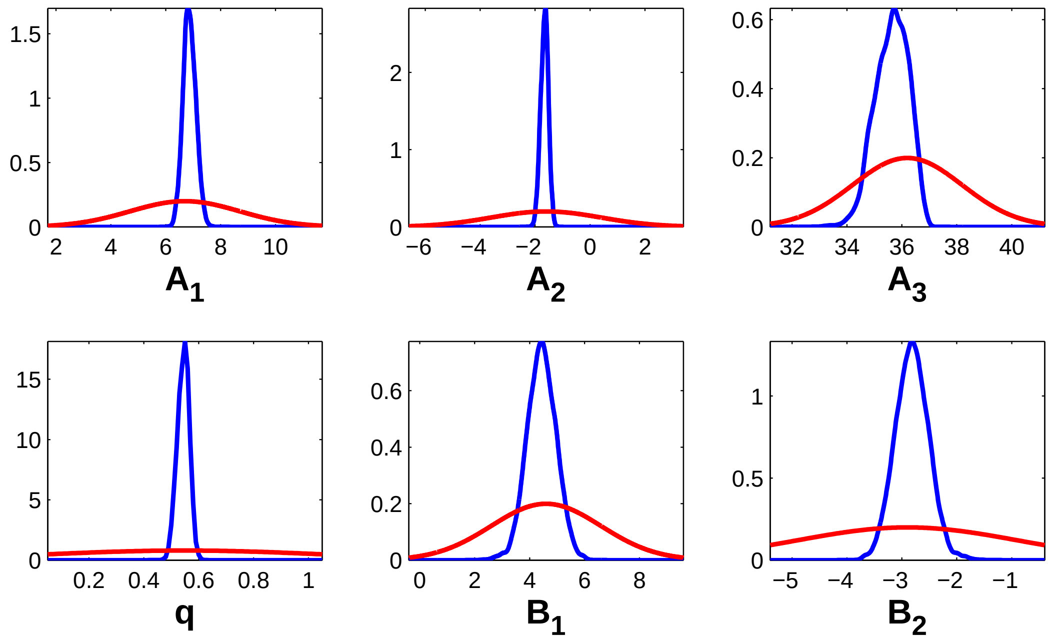

Figura 11: Prior densities (red line) and approximate marginal posterior densities (blue line) for A_1, A_2, q, B_1, B_2 and A_3. The estimated posterior densities for all parameters are more concentrated than the prior densities, which means that the data are informative. Again, the estimated posterior of q is highly concentrated. Allowing a non-constant variance has the effect of reducing the uncertainties of A_1, A_2 and the fatigue limit parameter, A_3. The estimated marginal posterior of the fatigue limit parameter is left-skewed although the prior was assumed to be a normal distribution.

Cuadro 10: MCMC posterior empirical mean estimates with their standard deviations.

	A_1	A_2	A_3	q	B_1	B_2
Mean	6.87	-1.66	35.63	0.544	4.44	-2.81
SD	0.23	0.14	0.60	0.022	0.53	0.31

informative for all the parameters as previously explained. The marginal posterior of the fatigue limit parameter, A_3 is left-skewed similar to the profile likelihood estimate. Correlation coefficients shown in Table 11 and Figure 12 show that A_1 and B_1 are almost perfectly correlated with A_2 and B_2, respectively. Thus, we can consider a fatigue limit model with non-constant variance with only four parameters, which is the same number of parameters in the logarithmic fit. The fatigue limit parameter in Model Ib has a moderate linear relationship with A_1, A_2 and q whereas the fatigue limit parameter in Model Ia has a strong linear relationship with A_1 and A_2 and a weak linear relationship with q.

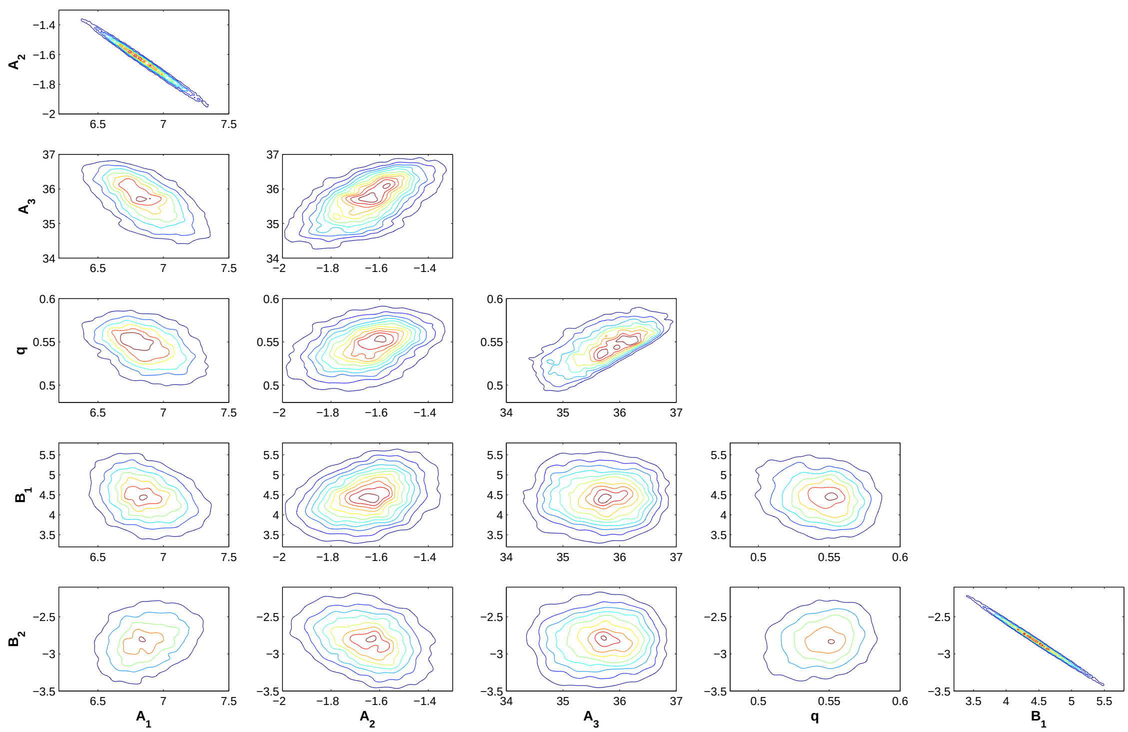

Figura 12: Contour plots of the approximate bivariate densities for each pair of parameters in Model Ib. There are two strong correlations between A_1 and A_2 and between B_1 and B_2. Such strong correlation suggests linear dependence; it is therefore possible to remove two parameters from Model Ib. The fatigue limit parameter, A_3, shows a moderate correlation with A_1, A_2 and q. Allowing a non-constant variance has the effect of increasing the correlation between q and the fatigue limit parameter, A_3.

Cuadro 11: Correlation coefficients for each pair of parameters in Model Ib.

	A_1	A_2	A_3	q	B_1
A_2	-0.993	—	—	—	—
A_3	-0.610	0.592	—	—	—
q	-0.384	0.396	0.658	—	—
B_1	-0.301	0.308	0.017	-0.177	—
B_2	0.300	-0.306	-0.011	0.188	-0.997

Numerical Results - Model IIb

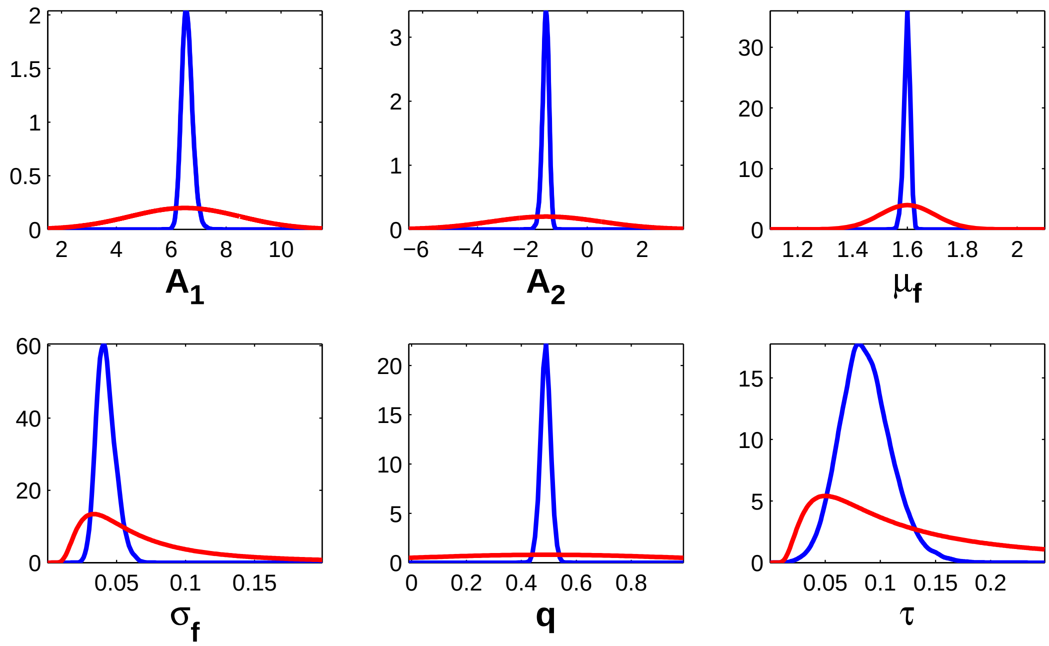

Figura 13: Prior densities (red line) and approximate marginal posterior densities (blue line) for A_1, A_2, q, τ, μ_f and σ_f. The posterior densities for all parameters are more concentrated than the prior densities, which means the data are informative. The high concentrations of the location and scale parameters, μ_f and σ_f, are particularly noticeable. The random fatigue-limit model has the effect of considerably reducing the uncertainties of A_1, A_2 and τ.

Maximum posterior estimates presented in Table 12 are similar to the maximum likelihood estimates obtained for Model IIb (Table 3). Figure 13 and Table 13 show that the

Cuadro 12: Maximum posterior estimates for Model IIb.

Estimator	A_1	A_2	μ_f	σ_f	q	τ
Laplace	6.51	-1.47	1.60	0.0387	0.488	0.082
Laplace-Metropolis	6.53	-1.49	1.60	0.0386	0.485	0.080

Cuadro 13: MCMC posterior empirical mean estimates with their standard deviations.

	A_1	A_2	μ_f	σ_f	q	τ
Mean	6.58	-1.52	1.60	0.0424	0.488	0.087
SD	0.20	0.12	0.012	0.007	0.018	0.023

location and scale parameters, μ_f and σ_f, are the least uncertain parameters. Moreover, the uncertainties have been reduced for A_1, A_2 and q when compared with Model Ia and Model Ib. Figure 13 shows that the data are very informative for all the parameters because there is a strong contraction between the prior densities and the posterior densities. Similarly to Model Ia, Table 14 and Figure 14 show that A_1 and A_2 are approximately linear dependent, and therefore we can reduce the number of parameters for Model IIb by one parameter. The location parameter, μ_f, is strongly correlated with A_1 and A_2 whereas σ_f is moderately correlated with A_1, A_2 and μ_f. There is a weak negative correlation between τ and σ_f and a weak positive correlation between τ and q.

Cuadro 14: Correlation coefficients for each pair of parameters in Model IIb.

	A_1	A_2	μ_f	σ_f	q
A_2	-0.986	—	—	—	—
μ_f	-0.777	0.708	—	—	—
σ_f	0.447	-0.404	-0.526	—	—
q	-0.045	0.090	-0.062	-0.145	—
τ	0.034	-0.022	0.042	-0.396	0.321

4.2. Model comparison

We now analyze more closely comparisons among models Ia, Ib and IIb.

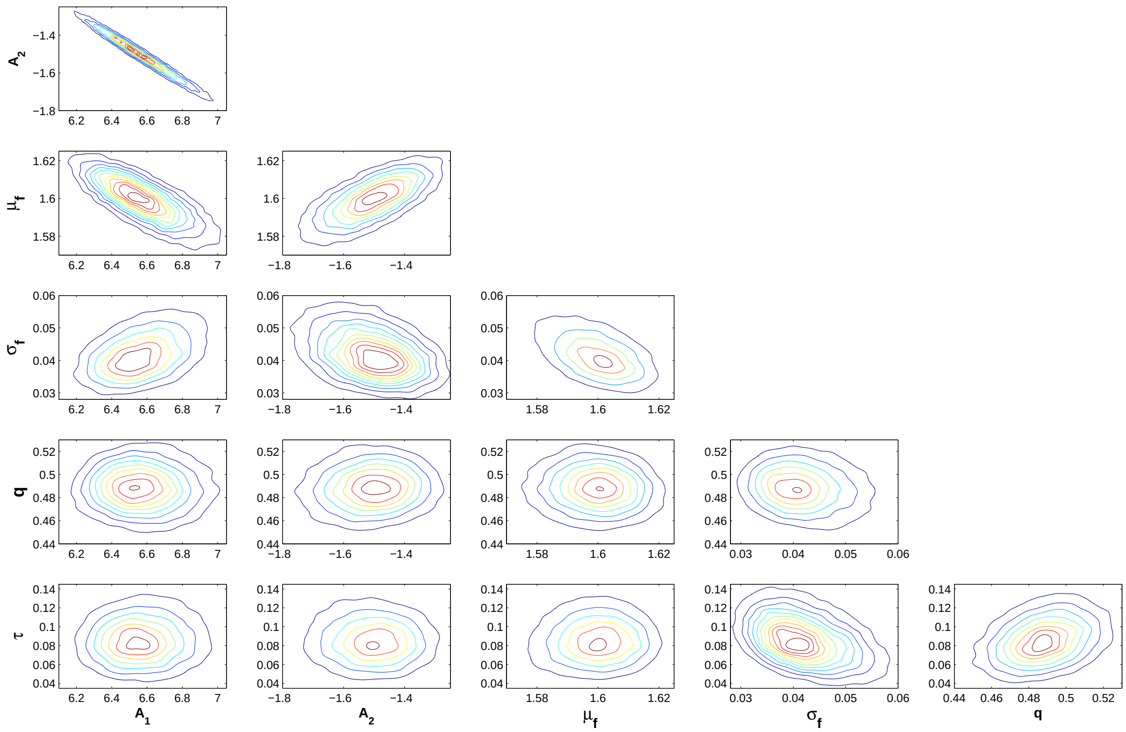

Figura 14: Contour plots of the approximate bivariate densities for each pair of parameters in Model IIb. Again, a strong correlation appears between A_1 and A_2. Also, the parameter μ_f has a relatively strong correlation with A_1 and A_2. The random fatigue-limit model has the effect of reducing the correlations between q and the parameters A_1 and A_2.

4.2.1. Bayes Factor

We adopt a traditional Bayesian approach by estimating the Bayes factor of Model A against that of Model B, which is defined as

$$F_{B,A} := \frac{\int L_B(\theta_B; \mathbf{y})\rho_B(\theta_B)d\theta_B}{\int L_A(\theta_A; \mathbf{y})\rho_A(\theta_A)d\theta_A} = \frac{p_B(\mathbf{y})}{p_A(\mathbf{y})},$$

where $\rho_A(\theta_A)$ and $\rho_B(\theta_B)$ are the prior densities, and $p_A(\mathbf{y})$ and $p_A(\mathbf{y})$ are the marginal likelihoods (Congdon, 2006, Chapter 2).

Common methods to estimate Bayes factors DiCiccio et al. (1997); Lewis and Raftery (1997) are applied to compare the fitted models and to rank their plausibility. Fast preliminary estimates of the log marginal likelihoods were obtained through the application of

the Laplace approximation. Then, the log marginal likelihoods were computed using the Laplace-Metropolis estimator, which is based on the MCMC posterior samples together with the Laplace approximation.
In both cases, the approximation of the log marginal likelihood $\log(p(\mathbf{y}))$ is given by

$$\frac{P}{2}\log(2\pi) + \frac{1}{2}\log(|H^*|) + \log\left(\rho(\theta^*)\right) + \log\left(L(\theta^*|\mathbf{y})\right),$$

where P is the dimension of the vector θ, θ^* is the maximum posterior estimate and H^* is the inverse Hessian of the negative log posterior.
In the Laplace estimator, θ^* and H^* are numerically approximated by means of the Broyden - Fletcher - Goldfarb - Shanno (BFGS) algorithm. The Laplace-Metropolis estimator uses the MCMC posterior samples to find the maximum posterior estimate, θ^*, and approximate, H^*, by the empirical covariance matrix.

4.2.2. Predictive Information Criteria for Bayesian Models

In this section, we compare models by measuring their prediction accuracy. We estimate the prediction accuracy using deviance and Watanabe-Akaike information criteria as well as cross-validation.

- **Log pointwise predictive density (lppd)**
  The general method to estimate the prediction accuracy of a certain model is through the log predictive density, $\log \rho(y|\theta) = \log L(\theta; y)$, where y is a new observation. An overestimate of the log predictive density can be obtained by using the observed data, $\{y_i\}_{i=1}^n$. It is an overestimate because the observed data were used first to infer θ. In our Bayesian approach, θ is summarized by the MCMC posterior samples, $\{\theta^m\}_{m=1}^S$, and therefore the log pointwise predictive density estimate is given by

  $$lppd = \sum_{i=1}^{n} \log\left(\frac{1}{S}\sum_{m=1}^{S}\rho(y_i|\theta^m)\right), \tag{5}$$

  where S should be "large enough" Gelman et al. (2014); Vehtari and Gelman (2014).

- **Deviance information criterion (DIC)**
  DIC can be considered as a Bayesian generalization of the AIC by replacing the maximum likelihood estimate by the posterior mean and computing the effective number of parameters, p_{DIC}, as follows:

  $$p_{\mathrm{DIC}} = 2\left(\log L(\bar{\theta}) - \frac{1}{S}\sum_{m=1}^{S}\log L(\theta^m)\right),$$

where $\bar{\theta}$ is the posterior mean Gelman et al. (2014). Then, the deviance information criterion is given by

$$\mathrm{DIC} = -2\left(\log L(\bar{\theta}) - p_{DIC}\right).$$

- **Watanabe-Akaike information criterion (WAIC)**
WAIC or widely applicable information criterion is a stable Bayesian predictive measure that approximates the leave-one-out cross-validation (see Gelman et al. (2014),
Vehtari and Gelman (2014); Watanabe (2010)) and is defined by

$$p_{\mathrm{WAIC}} = 2\sum_{i=1}^{n}\left(\log\left(\frac{1}{S}\sum_{m=1}^{S}\rho(y_i|\theta^m)\right) - \frac{1}{S}\sum_{m=1}^{S}\log\rho(y_i|\theta^m)\right),$$

$$\mathrm{WAIC} = -2(lppd - p_{\mathrm{WAIC}}).$$

- **K-fold cross-validation**
Cross-validation is the most popular yet computationally expensive method to estimate a model's predictive accuracy. We consider the K-fold cross-validation where the data are randomly partitioned into K disjoint subsets, $\{\mathbf{y}_k\}_{k=1}^{K}$. Then, we define $\{\mathbf{y}_{(-k)}\} = \{\mathbf{y}_1, \ldots, \mathbf{y}_{k-1}, \mathbf{y}_{k+1}, \ldots, \mathbf{y}_K\}$ to be a training set. For each training set, we compute the corresponding posterior distribution, $p(\theta|\mathbf{y}_{(-k)})$. Then, the log predictive density for $y_i \in \mathbf{y}_k$ is computed using the training set $\{\mathbf{y}_{(-k)}\}$, that is:

$$lpd_i = \log\left(\frac{1}{S}\sum_{m=1}^{S}\rho(y_i|\theta^{k,m})\right), i \in k,$$

where $\{\theta^{k,m}\}_{m=1}^{S}$ are the MCMC samples of the posterior $p(\theta|\mathbf{y}_{(-k)})$. Finally, we sum to obtain the expected log predictive density (elpd):

$$elpd = \sum_{i=1}^{n} lpd_i.$$

The K-fold cross-validation (with $K = 5$ or 10) is usually used instead of the leave-one-out cross-validation, which is the most computationally exhaustive type of cross-validation (see (Izenman, 2008, Chapter 5) and Vehtari and Gelman (2014)).

In the next Subsection, we present the main numerical results from applying the techniques described in Subsections 4.2.1 and 4.2.2 for Models Ia, Ib and IIb under the predefined scenario.

Cuadro 15: Log marginal likelihoods (Bayes factors) show very strong evidence that Model Ib is better than Model Ia and that Model IIb is better than Model Ib. The predictive information criteria and the 5-fold cross-validation show that Model IIb also has better predictive accuracy than do Model Ia and Model Ib.

Models	**Model Ia**	**Model Ib**	**Model IIb**
Log marginal likelihood (Laplace)	-963.07	-940.18	-932.55
Log marginal likelihood (Laplace-Metropolis)	-963.16	-937.06	-923.68
Log pointwise predictive density (lppd)	-949.56	-920.51	-907.85
Deviance information criterion (DIC)	1909.6	1851.8	1826.5
Watanabe-Akaike information criterion (WAIC)	1911.3	1853.1	1825.9
5-fold cross-validation elpd	-955.42	-927.07	-913.80

4.2.3. Numerical Results (Informative priors scenario)

Table 15 shows that Model IIb under the informative priors scenario is preferable by the log marginal likelihood and the predictive information criteria. The Laplace method appears to underestimate the log marginal likelihood for Model IIb. This is expected because of the complex likelihood function of Model IIb and because the Gaussian approximation does not always provide a good estimation. Table 15 also shows consistency with the classical information criterion presented in Table 5.

5. Conclusions and future work

We calibrated models of various complexity that were designed to account for right-censored data by means of the maximum likelihood method. We used a data set described in Section 2 for this purpose. The robustness of the estimation of the quantile functions has been assessed by computing bootstrap confidence intervals for samples stratified with respect to the cycle ratio.

We then considerably enlarged the scope of our study by considering a Bayesian approach. Any prior distribution, which is suitable to describe the available knowledge on the physical parameters, can be easily incorporated into our Bayesian computational framework that provides a simulation-based posterior distribution.

To decide which model could be considered more reliable for deployment, first we computed classical measures of fit based on information criteria. Then, the Bayesian approach for model comparison was applied to determine which model would be preferred under any prescribed a priori scenarios. Here we examined the informative priors scenario. This approach included very different techniques ranging from those based on the estimation

of the marginal likelihood to those based on predictive information criteria, whose implementation requires the use of cross-validation techniques.
The classical approach and the Bayesian approach for model comparison have provided evidence in favor of Model IIb given the 75S-T6 data set described in Section 2. Model IIb assumes that both fatigue life and the fatigue limit parameter follow a Weibull distribution and the expected value of the fatigue limit parameter, A_3, is 39.88 ksi.
An integrated set of computational tools has been developed for model calibration, cross-validation, consistency and model comparison, allowing the user to rank alternative statistical models based on objective criteria.
A natural extension of this work is the study of fatigue life prediction of metallic materials with small notches. Several predictors of damage accumulation, i.e. phenomenological models constructed for the purpose of generalizing sets of experimental data obtained in fatigue tests of mechanical or structural components subjected to cyclic loading, have been recently proposed in Szabó et al. (2016), together with a schematic procedure to provide their objective ranking. Stochastic models for crack initiation will be developed, at a first instance, in a realistic three-dimensional setting on the basis of the S-N curves that must be calibrated for any selected type of metallic material.

Acknowledgement

Z. Sawlan, M. Scavino and R. Tempone are members of King Abdullah University of Science and Technology (KAUST) SRI Center for Uncertainty Quantification in Computational Science and Engineering.

Referencias

Akaike, H. (1992). Information theory and an extension of the maximum likelihood principle. In *Breakthroughs in Statistics, Volume I*, pages 610–624. Springer.

Bathias, C. (1999). There is no infinite fatigue life in metallic materials. *Fatigue and Fracture of Engineering Materials and Structures*, 22(7):559–566.

Berger, J. (2006). The case for objective Bayesian analysis. *Bayesian Analysis*, 1(3):385–402.

Burnham, K. P. and Anderson, D. R. (2002). *Model Selection and Multimodel Inference*. Springer, second edition.

Castillo, E. and Fernández-Canteli, A. (2009). *A Unified Statistical Methodology for Modeling Fatigue Damage*. Springer.

Congdon, P. (2006). *Bayesian Statistical Modelling.* John Wiley & Sons, second edition.

DiCiccio, T. J., Kass, R. E., Raftery, A., and Wasserman, L. (1997). Computing Bayes factors by combining simulation and asymptotic approximations. *Journal of the American Statistical Association*, 92(439):903–915.

Efron, B. (1981). Censored data and the bootstrap. *Journal of the American Statistical Association*, 76(374):312–319.

Fatemi, A. and Yang, L. (1998). Cumulative fatigue damage and life prediction theories: a survey of the state of the art for homogeneous materials. *International Journal of Fatigue*, 20(1):9–34.

Gelman, A., Hwang, J., and Vehtari, A. (2014). Understanding predictive information criteria for Bayesian models. *Statistics and Computing*, 24(6):997–1016.

Grover, H. J., Bishop, S. M., and Jackson, L. R. (March 1951). *Fatigue Strengths of Aircraft Materials. Axial-Load Fatigue Tests on Unnotched Sheet Specimens of 24S-T3 and 75S-T6 Aluminum Alloys and of SAE 4130 Steel NACA TN 2324.* National Advisory Committee on Aeronautics.

Izenman, A. J. (2008). *Modern Multivariate Statistical Techniques.* Springer.

Lewis, S. M. and Raftery, A. E. (1997). Estimating Bayes factors via posterior simulation with the Laplace–Metropolis estimator. *Journal of the American Statistical Association*, 92(438):648–655.

Meeker, W. Q. and Escobar, L. A. (1998). *Statistical Methods for Reliability Data.* John Wiley & Sons.

Neath, A. A. and Cavanaugh, J. E. (2012). The Bayesian information criterion: background, derivation, and applications. *Wiley Interdisciplinary Reviews: Computational Statistics*, 4(2):199–203.

Pascual, F. G. and Meeker, W. Q. (1997). Analysis of fatigue data with runouts based on a model with nonconstant standard deviation and a fatigue limit parameter. *Journal of Testing and Evaluation*, 25:292–301.

Pascual, F. G. and Meeker, W. Q. (1999). Estimating fatigue curves with the random fatigue-limit model. *Technometrics*, 41(4):277–289.

Pawitan, Y. (2001). *In All Likelihood: Statistical Modelling and Inference Using Likelihood.* Oxford University Press.

Pyttel, B., Schwerdt, D., and Berger, C. (2011). Very high cycle fatigue–is there a fatigue limit? *International Journal of Fatigue*, 33(1):49–58.

Rice, R. C., Jackson, J. L., Bakuckas, J., and Thompson, S. (2003). *Metallic Materials Properties Development and Standardization (MMPDS-01) Handbook*. Battelle Memorial Institute.

Robert, C. and Casella, G. (2009). *Introducing Monte Carlo Methods with R*. Springer.

Ryan, K. J. (2003). Estimating expected information gains for experimental designs with application to the random fatigue-limit model. *Journal of Computational and Graphical Statistics*, 12(3):585–603.

Schijve, J. (2003). Fatigue of structures and materials in the 20th century and the state of the art. *International Journal of Fatigue*, 25(8):679–702.

Schijve, J. (2009). *Fatigue of Structures and Materials*. Springer, second edition.

Schwarz, G. (1978). Estimating the dimension of a model. *Ann. Statist.*, 6(2):461–464.

Shampine, L. F. (2008). Vectorized adaptive quadrature in MATLAB. *Journal of Computational and Applied Mathematics*, 211(2):131–140.

Szabó, B. (August 2012). *Private Communication*.

Szabó, B., Actis, R., and Rusk, D. (2016). Predictors of fatigue damage accumulation in the neighborhood of small notches. *International Journal of Fatigue*, 92(1):52–60.

Vehtari, A. and Gelman, A. (2014). Waic and cross-validation in Stan.

Walker, K. (1970). The effect of stress ratio during crack propagation and fatigue for 2024-t3 and 7075-t6 aluminum. *Effects of environment and complex load history on fatigue life*, 462:1–14.

Watanabe, S. (2010). Asymptotic equivalence of Bayes cross validation and widely applicable information criterion in singular learning theory. *Journal of Machine Learning Research*, 11:3571–3594.

Instituto de Estadística

Documentos de Trabajo

Eduardo Acevedo 1139. CP 11200 Montevideo, Uruguay
Teléfonos y fax: (598) 2 410 2564 - 2418 7381
Correo: ddt@iesta.edu.uy
www.iesta.edu.uy
Área Publicaciones

Marzo, 2016
DT-1/2016